8

Junction Properties and Applications of ZnO Single Nanowire Based Schottky Diode

Sachindra Nath Das[1], Jyoti Prakash Kar[2] and Jae-Min Myoung[2]
[1]*Department of Physics, Burdwan Raj College, Burdwan, West Bengal,*
[2]*Department of Material Science and Engineering, Yonsei University, Seoul,*
[1]*India*
[2]*South Korea*

1. Introduction

Towards the beginning of 21st century, considerable interests have been paid to synthesize low-dimensional nanostructures, such as nanowires, nanorods or nanobelts because of their unique structures with large surface-to-volume ratio. Nanodevice units made from those one-dimensional nanostructures (single nanostructures as well as bunch of nanostructures) have attracted substantial research interests because they provide a unique platform for fundamental investigations. In addition, they can also serve as the building blocks for more complicated nano-systems and micro-systems, for example, sensors, diodes, solar cells, LEDs, nano-generators and transistors (Lee et al., 2010; Zhou et al., 2008). Recently, many successful attempts to develop nano-devices by using different nanostructures have already been described in scientific literatures.

There has been steady progress in demonstrating electrical components made of nanowires, such as field effect transistors, electron field emitters, switches, sensors, etc. The surface of the nanostructures has crucial role in determining the electrical and optoelectronic properties of nano-devices. As the surface-to-volume ratio is very high, the surface states also play a key role on optical absorption, gas sensing, luminescence and other properties. Thus, nanoscale electronic devices have the potential to achieve higher sensitivity and faster response than bulk material. Most of these applications require metal contact to receive and/or transmit electrical signals or to be powered by an external source. So, the devices with nanowires, nanorods or nanobelts, the electrical contacts should be scaled accordingly. Thus, the understanding of transport processes at the nanometer scale is essential for an overall improvement of the device characteristics.

Depending on the Fermi surface alignment and the nature of the interface between the metal and the semiconducting nanowires, the contacts can either be an Ohmic contact or a Schottky contact. Whether a contact is a Schottky or ohmic, depends on the work-function (Φ) of the metal and the semiconducting nanowire and also on the type of majority carriers (electrons or holes). For n-type semiconductor, if the work function of the metal (Φ_M) used for contact is higher than that of the semiconductor (Φ_S), a Schottky barrier will be formed. According to the Schottky-Mott theory, the barrier height (Φ_B) follows the rule ($\Phi_B = \Phi_M - \chi_S$),

where χ_S is electron affinity of semiconductor. But, in case of low dimensional system, the Schottky barrier height depends not only on the work functions of the metal and the semiconductor nanowire, but also on the pinning of the Fermi level by surface states, image force lowering, field penetration and the existence of an interfacial insulating layer. To a good approximation, all of these effects change only the absolute current value at very low bias regime via lowering the Schottky barrier. Thus, detailed study on Schottky nanocontacts are important because not only a great number of nanodevices are based on a metal/semiconductor Schottky contact with nanometer dimensions, but also standard electrical spectroscopies, such as deep level transient spectroscopy or photocurrent measurements, need the formation of Schottky contact. Metal/semiconductor Schottky device is also one of the most fundamental one that can be used to evaluate various semiconductor parameters including carrier density and Schottky barrier height as well as carrier density profile and bandgap discontinuity.

In this context, several semiconducting materials, such as GaN, ZnO, and AlGaN, have wide direct bandgaps which make them useful for electronic and optoelectronic applications. Among these materials, growth of vertically aligned single crystalline ZnO nanowires is easier. It is a direct wide bandgap (3.37 eV) piezoelectric material with hexagonal wurtzite structure, and has larger exciton binding energy (60 meV) than other wide bandgap semiconductor (GaN, 25 meV). Moreover, single crystalline nanowires have attracted a lot of interest for the fabrication of nanoelectronic and nanophotonic devices due to their extraordinary properties originated from their high crystallinity and large aspect ratio.

In this chapter, we have described the junction properties of ZnO nanowire based Schottky diodes with different contact metal. Also we have described the UV detection and gas sensing mechanism of single nanowire based Schottky diode which will further promote an understanding of the device physics and practical applications.

2. ZnO nanowire

Vertically aligned ZnO nanowires with controlled shape and ordered surface morphology have attracted considerable attentions due to their low dimensional structures and the exciting prospects for utilizing these materials in nanotechnology enabled electronic and photonic crystal device applications (Zhang et al., 2001; Chang et al. 2009). As a wide bandgap (~3.4 eV) semiconductor, ZnO has drawn a great interest for low-voltage and short wavelength optoelectronic devices (Norton et al., 2004). It is expected that in ZnO nanowires, one may eliminate some unwanted properties of bulk ZnO, such as weak exciton emission in comparison with the defect related (deep-level) visible emission, while keeping or enhancing the desirable properties such as large exciton binding energy (60 meV) (Fonoberov et al., 2006).

2.1 Nanowire growth

In order to control shape, aspect ratio (length/width), growth site and growth direction of the nanowires, many efforts have been directed towards the synthesis of ZnO nanostructures by aqueous, vapor–liquid–solid (VLS), metal organic chemical vapor deposition (MOCVD) and many other techniques (Kar et al.,2008; 2009; Hsu et al., 2005). However, MOCVD method is of particular interest since it has some advantages such as the

ability to fabricate nanostructures of better quality, well controllable configurations and good reproducibility. As the growth of ZnO nanowires by MOCVD is a bottom-up technique, the nature of substrates has a vital role for the dimension and alignment of the nanowires. According to lattice misfit, the most suitable substrate for ZnO growth is $ScAlMgO_4$, which is expensive and technologically inconvenient (Ievtushenko et al., 2008). On the other hand, it is difficult to obtain well-aligned ZnO nanowires on silicon substrates, because the formation of an interfacial layer (SiO_2) and large lattice misfit (Liou et al., 2005). Interestingly, C-plane sapphire overcomes some of the limitations arising from the above substrates. The ZnO nanowires, used in the experiments, were grown on *c*-plane sapphire substrates without any catalyst by using MOCVD system. Diethyl zinc and high purity oxygen (5N) were used as the Zn and O sources, respectively. The base pressure of the reactor chamber and the working pressure were kept at 10^{-6} Torr and 3 Torr, respectively. During the growth, the nozzle-substrate spacing was 1 cm and the substrate temperature was fixed at 700 °C.

2.2 Micro-structural and optical property

Fig. 1(a) shows a typical FESEM image of vertically aligned ZnO nanowires (diameter~100 nm) grown on c-plane sapphire substrate. The appearance of a prominent (002) peak in XRD pattern (not shown here) confirms the crystalline natures of ZnO nanowires. Fig. 1(b) shows the bright field TEM image of a ZnO nanowire. The diameter of the nanowire is around 100 nm and uniform through out its length. In order to further investigate the structural characteristics of ZnO nanowire, high-resolution transmission electron microscopy (HRTEM) experiment was carried out and the magnified image is shown in the inset of Fig. 1(b). HRTEM images at different part of nanowire indicate that the nanowire is structurally uniform and do not exhibit any noticeable defects. Furthermore, the HRTEM image confirmed that the single crystalline ZnO nanowire is preferentially oriented along the c-axis direction with lattice spacing of 0.52 nm. The selective area electron diffraction (SAED) pattern (inset of Fig. 1(b)) also shows that the nanowire exhibits a single crystalline nature. These results are almost consistent with the FESEM observation.

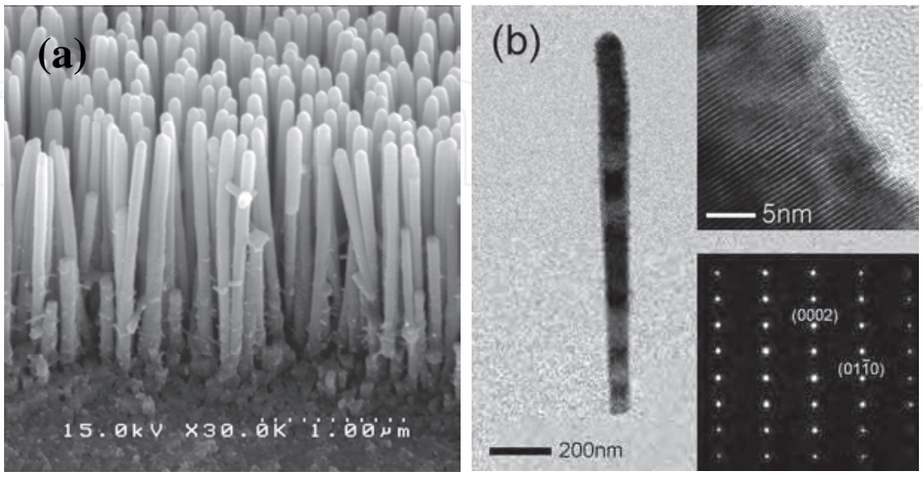

Fig. 1. (a) FESEM images and (b) TEM images of ZnO NR arrays. Inset shows the corresponding HRTEM images and diffraction pattern.

Information such as surface oxygen vacancies and other defects as well as the separation and recombination of photoinduced charge carriers can be obtained from photoluminescence (PL) measurements. Fig. 2 presents the low temperature (10 K) PL spectrum of dispersed ZnO NWs measured with 325 nm He-Cd laser. In our NWs, two strong PL peaks at 382 and 388 nm were found without any visible band emission.

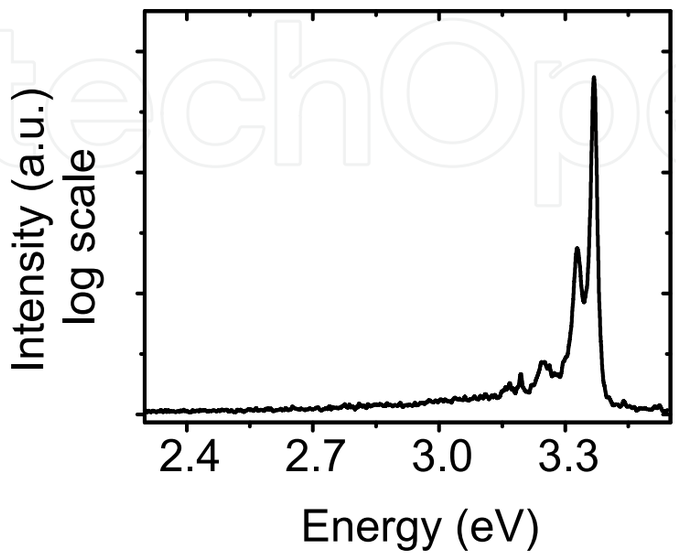

Fig. 2. Photoluminescence spectra (10 K) of ZnO nanowire arrays.

3. Junction properties

3.1 Fabrication of single nanowire device

Electrical contacts to individual nanowires were fabricated using a procedure of lithography, metallization and lift-off technique. The nanowires were first removed from the substrate and then dispersed by sonication in isopropanol. A droplet of dispersed solution containing nanowires was then dropped on photo-lithographically pre-assigned metallic micro-pads on the substrate. Thermally oxidized (500 nm) Si wafers were used as substrates for the fabrication of Schottky diodes. The coordinates of several nanowires with respect to the pre-assigned metallic pads were then estimated by using Scanning Electron Microscope (SEM). Finally, the path of electrical connections between the pre-assigned micro-pads and the nanowires were made by e-beam lithography and lift-off techniques. All metals were deposited by Ar plasma assisted DC sputtering at a pressure of 3 mTorr. The contacts were patterned by lift-off of lithographically defined photo-resist.

To form Ohmic contact 100 nm of Ti and 200 nm of Au were successively deposited on one side of the nanowire followed by rapid thermal annealing at 550 ^{o}C for 1 min in N_2 atmosphere. In addition, to form Schottky contact metal with higher work function (Au, Pt or Ni) was deposited (300 nm) on the other side of the nanowire. The devices were also fabricated with homogeneous ZnO nanowire and Ti/Au contacts on both sides by using the same experimental procedures and they have shown linear current voltage (*I-V*) characteristics, confirmed the ohmic contacts with ZnO nanowire. The schematic diagram and the FESEM image of single ZnO nanowire based device are shown in Fig. 3 (a) and (b), respectively.

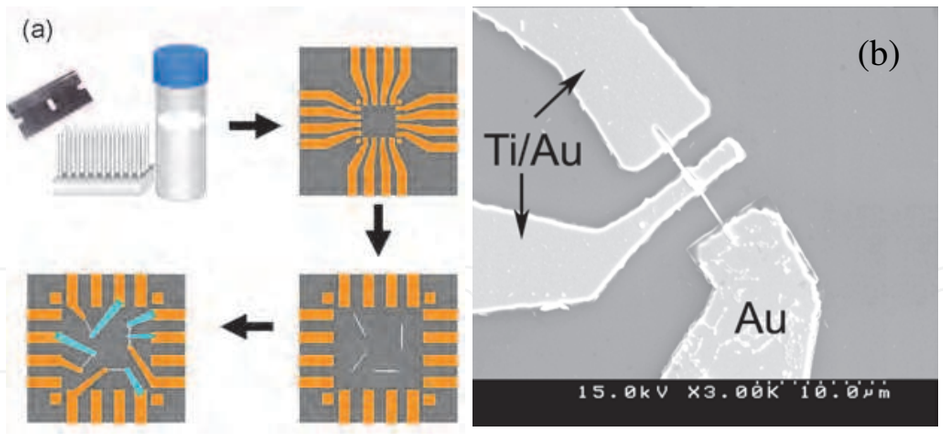

Fig. 3. (a)The schematic diagram and (b) FESEM image of single ZnO NW based device.

3.2 Electrical characterization

In case of low dimensional systems, the Schottky barrier height depends not only on the work functions of the metal and the semiconductor nanowire, but also on the pinning of the Fermi level by surface states, image force lowering, field penetration and the existence of an interfacial insulating layer. To a good approximation, all of these effects change only the absolute current value via lowering the Schottky barrier. The temperature dependent *I-V* characteristics of Schottky Diodes, fabricated with Au, Pt and Ni metal were investigated and their typical characteristics are shown in Fig. 4 (a), (b) and (c), respectively. It is also found that the *I-V* curves are nonlinear, asymmetrical and exhibit clear rectifying behavior for all the measured temperatures. The current under forward bias increases with temperature and shows typical semiconductor characteristics. The electrical characterization of Schottky diode necessitates the determination of the barrier height and the ideality factor. Generally, total current consists of both thermionic emission and tunneling component. Assuming that the thermionic emission is the most predominant mechanism, the general form of the temperature dependence of current may be expressed as (Sze, S.M. 1979):

$$I = AA^{*}T^{2}\exp\left(-\beta\Phi_{B}\right)\exp\left[\frac{\beta\left(V-IR\right)}{n}\right] \tag{1}$$

where, Φ_B is the effective barrier height, A is the junction area, A^* [$A^* = 4\pi qm^*k^2/h^3$] is the Richardson constant and m^* is the effective mass of the charge carriers. R is the series resistance and $\beta = q/kT$. For an ideal diode, the diode ideality factor (n) should be nearly equal to unity. But in a real situation, it may increase when the effects of series resistance, leakage current etc. come into play. The main difficulty of the thermionic emission theory is that it underestimates the reverse current. But the situation is very different in a nano-system, where the measured forward current is low and is comparable to that of the reverse or leakage current. The tunneling current is therefore not negligible and indeed becomes the dominating mechanism under reverse bias. Also there are inherent difficulties when the base material would offer a considerable series resistance, which would cause a voltage drop across the junction. The current flows according to thermionic emission model only when the ideality factor (n) is near unity. With an increase in n, the barrier height would deviate from the true value. For the large surface-to-volume ratio of the ZnO nanowire, the

surface states and the effective carrier concentration have important influence to the contact barrier. The variation of oxygen and zinc concentration during the growth of the nanowire results in the nonuniform distribution of the defects. A slight inhomogeneity of the surface states and carrier concentration at the two ends of the ZnO nanowire can result in different Schottky barriers. In such a case, generalized Norde method could be used to evaluate the effective barrier height, series resistance, and diode ideality factor (n) from I–V measurement. The values of effective barrier potential and diode ideality factor measured at different temperatures for Au/n-ZnO/Ti-Au, Ni/n-ZnO/Ti-Au and Pt/n-ZnO/Ti-Au Schottky diodes are shown graphically in Fig. 5 (a) and (b), respectively.

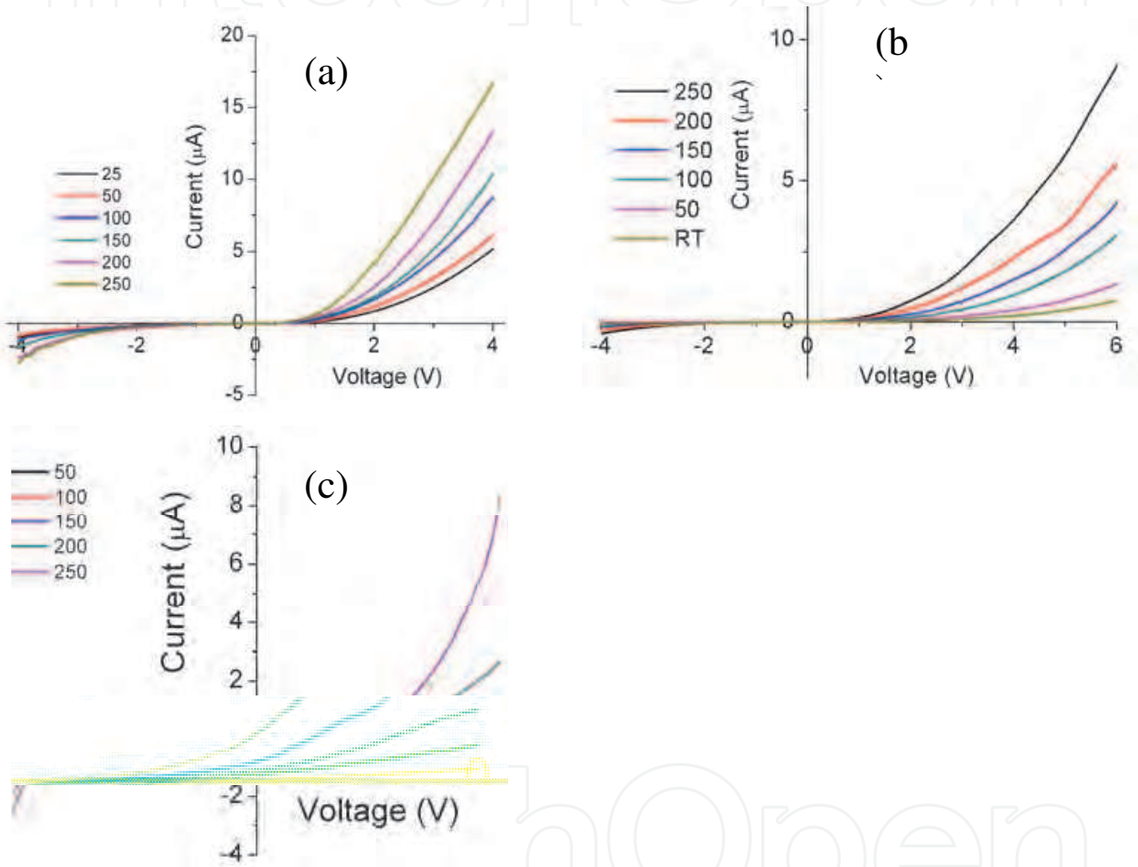

Fig. 4. I-V characteristics of (a) Au/n-ZnO, Ni/n-ZnO and Pt/n-ZnO Schottky diode measured at different temperature.

The barrier height could be seen to increase with temperature (Fig. 5(a)) almost linearly. Pt offered larger barrier height than that offered by Au and Ni while Au and Ni contacts indicated nearly similar barrier heights. The increase in barrier heights with the increase in temperature from 300 K to 523 K may be associated with the increase in available charge carriers to be transported across the barrier for Fermi level equalization. It is also observed that the values of barrier heights obtained from the I–V characteristics were lower than those obtained for a thin-film based Schottky diodes. Lower values of barrier height were ascribed to an enhanced electric field at the depletion region due to the small size of the nano-Schottky junction.

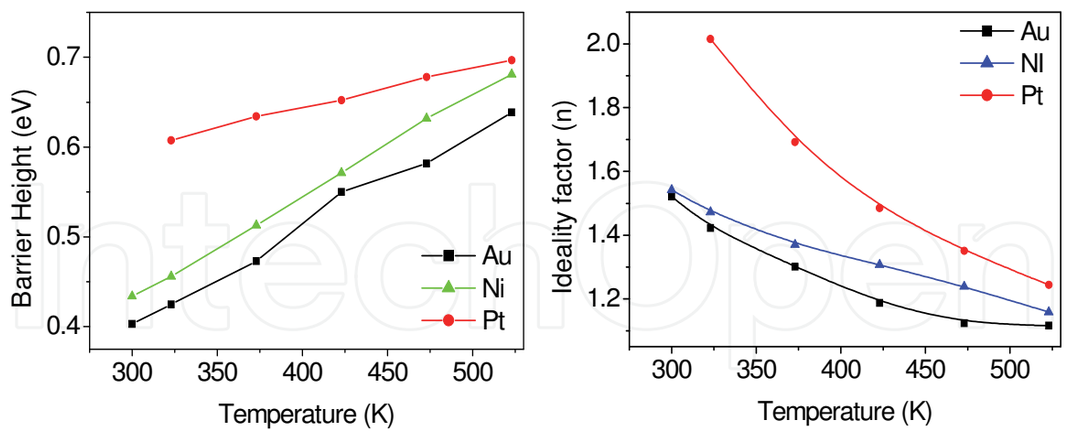

Fig. 5. Variation of (a) barrier height (Φ_B) and (b) ideality factor (n) with temperature (K).

Ideality factor for the different Schottky diodes studied here varied between 1.1 and 2.0. Schottky diodes with Au Schottky contact indicated lower ideality factor (~1.5) at room temperature than that for Ni and Pt. It may be observed that the ideality factor decreased with increasing temperature. Current transport across the metal semiconductor interface is temperature dependent. Thus, the electrons at low temperature would be able to cross only the lower barriers and therefore current transport will be dominated by current passing through the lower Schottky barrier only contributing to a large ideality factor. With increasing temperature, more and more electrons would acquire significant energy to cross higher barrier. As a result, the effective barrier height will increase with the temperature and bias voltage culminating in lower ideality factor at higher temperature. This increment can be explained by taking into account of the interface state density distribution, quantum mechanical tunneling and image force lowering across the barrier of Schottky diodes.

3.3 XPS studies

In order to further confirm the barrier-height value of nanowire Schottky diodes, XPS is used to study the surface Fermi level position within the band gap for metallic overlayer on ZnO nanowire. Each element has a characteristic binding energy for its core electrons, and thus each element has a characteristic spectrum. Comparison of the spectrums of a bare specimen, such as ZnO, and a specimen with a thin film coating, such as ZnO/Au, can yield the barrier height of the surface. The barrier height was determined from the XPS data using the following relation (Lin, 2005)

$$q\varphi_n = E_G - E_V^i + \left(E_{core}^i - E_{core}^{Au}\right) = E_G - \left(E_{core}^{Au} - E_{VC}\right) \tag{2}$$

where E_G is the bandgap of ZnO, E_V^i is the initial binding energy, E_{core}^i is the initial binding energy of the core level, E_{core}^{Au} is the binding energy of the core level with Au over layer and E_{VC} is equal to (E_{core}^i - E_V^i). All the binding energies are compared to E_F . Fig. 6(a) shows the Zn 3d core level and the valance band spectrum of ZnO nanowires. The value of E_{VC} is calculated to be 7.53 eV. This is in good agreement with the reported value (Tsai et al. 2009). Fig. 6(b) shows the Zn 3d core level at Au/ZnO nanowire interface. The spectra determine

the Zn 3d binding energy E_{core}^{Au} (10.48 eV) relative to the E_F. Therefore, the $q\Phi_n$ was calculated to be 0.42 eV. This is similar to the value (0.40 eV) obtained from *I-V* measurements at 300 K.

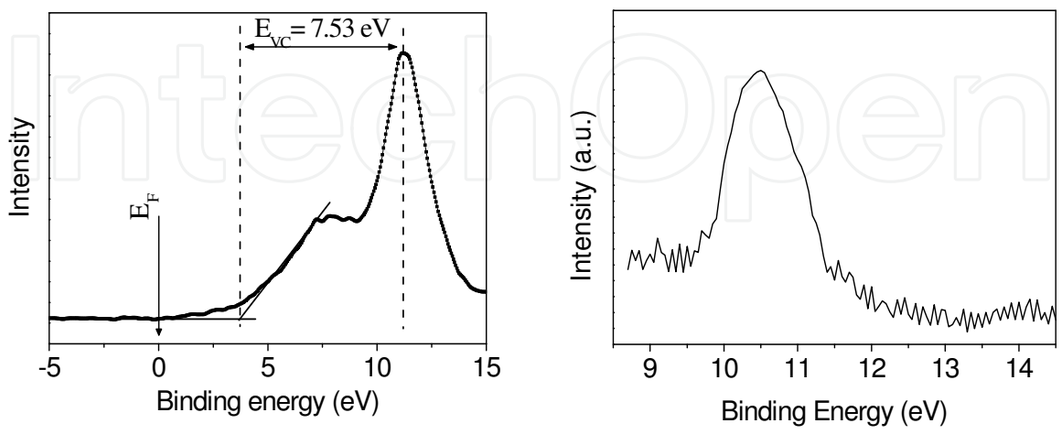

Fig. 6. (a) Zn 3d core level peak of ZnO nanowire without Au over-layer. The low energy region represents the spectrum of valance band region. A linear fit is used to determine the the energy of the valance band edge. (b) Zn 3d core level at the Au/ZnO nanowire interface.

3.4 Possible explanation

The deviations of diode ideality factor from unity signify the inhomogeneous nature of the Schottky diodes. Assuming the Gaussian distribution for Schottky barrier height (Φ_{B0}), the apparent barrier height (Φ_{ap}) can be written as (Werner et al., 1991; Bengi et al., 2007).

$$\Phi_{ap} = \Phi_{B0}(T=0) - \frac{q\sigma_0^2}{2kT} \tag{3}$$

where, σ_0 is the measure of the barrier homogeneity. The lower value of σ_0 corresponds to more homogeneous barrier height. The value of σ_0 obtained for temperatures for Au/*n*-ZnO/Ti-Au, Ni/*n*-ZnO/Ti-Au and Pt/*n*-ZnO/Ti-Au Schottky diodes are (from Fig. (7)) 0.112 V, 0.112V and 0.102 V, respectively. The values are quite low but not negligible compared to the apparent barrier height. Considering Au/n-ZnO schottky contact for details study, the calculated value of barrier height, obtained from the thermionic emission model and XPS measurement, is lower than the theoretically predicted value ($q\Phi_B = \Phi_M - \chi_S$ = 1.2 eV) and that reported for thin film based Schottky diodes ($q\Phi_B$ = 0.7-0.9 eV) (Angadi et al., 2007; Coppa et al., 2003; Dhananjay et al., 2007). This discrepancy is partly due to the effects of tunneling, image force lowering on the conduction process, surface defect states, barrier height inhomogeneities and moreover Fermi level pinning in nanowires. In addition, edge leakage current due to a high electric field at the metal contact periphery or interface current due to traps at the metal semiconductor interface also affect the barrier height. Other effects due to interface oxide layer between the Ti/ZnO contacts may also contribute to such deviations.

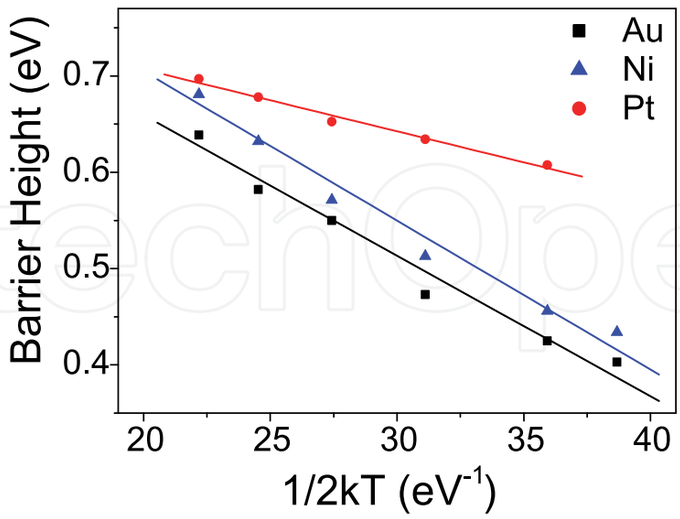

Fig. 7. Plot of Φ_{ap} versus 1/2kT.

In order to understand the lowering in Schottky barrier height, we also have to know the electronic transport mechanism, which can be deduced from temperature dependent *I-V* characteristics. In the presence of tunneling, *I* can be written as (Sze, S. M. 1979; Lin Y. J., 2005)

$$I = I_0 \exp\left(\frac{eV}{E_0}\right) \tag{4}$$

where the saturation current (I_0) is given by

$$I_0 = \frac{AA^*\left[\pi E_{00} q\left(\varphi_B - V - \xi\right)\right]^{0.5}}{k_B \cosh\left(E_{00}/k_B T\right)} \exp\left(-\frac{e\xi}{k_B T} - \frac{e\left(\varphi_B - \xi\right)}{E_0}\right) \tag{5}$$

In equation (5) ξ, [= (E_C-E_F)/q = (0.2 V)] obtained from ultraviolet photoelectron spectroscopy (UPS) measurement (not shown here), is the difference between the conduction band minimum and the position of the Fermi level, $E_0 = E_{00} \coth(E_{00}/k_BT)$ is the characteristic energy related to the tunneling probability and E_{00} is the tunneling parameter. In our case, E_{00} is 50 and 60 meV at 300 and 523 K, respectively, which is about 2 times higher than the thermal energy (25 and 43 meV at 300 and 523 K, respectively). As the temperature increases, the thermionic emission increases but the tunneling process is temperature insensitive. This result clearly supports that tunneling has a significant role at the forward current and thermionic-field emission (TFE) process is the main mechanism in Au/ZnO nanowire Schottky diode.

Although the image force lowering ($\Delta\Phi_B$), ascribed for enhanced electric field at the depletion region due to small size of the nano-Schottky junction, contributes to the barrier height reduction, the tunneling effect is also significant for nanocontact. But, only the image force lowering ($\Delta\Phi_B$=0.06 V, considering $\varepsilon_s = 2\varepsilon_0$ and electric field at nanocontact =10^4 V/cm), inhomogeneity in barrier height ($\Delta\Phi_B$=0.11 V) and tunneling are not enough to explain the difference between the theoretically predicted value and obtained experimental result. The

surface states play a key role on luminescence and optical absorption properties when the surface-to-volume ratio is high. The states, inside the bandgap, are formed on the ZnO surface due to Zn or O termination, dangling bonds, surface reconstruction or relaxation, structural and point defects, etc. When the diameter of nanowires becomes more than 30 nm, surface states also remain active. However, their relative contribution to the emission spectrum is small in comparison to the contribution originating from the grain volume. To explain this discrepancy, one may consider the effect of defect states at ZnO nanowire surface. But in that case, high density of defect states are required which is inconsistent with the small reverse leakage current in the device and observed photoluminescence property of our as deposited nanowire arrays (Das et al., 2009).

Generally, the band level alignment can be organized in two regimes: Fermi level pinning and vacuum level alignment (i.e, the Schottky-Mott limit). For nanowires, in absence of the metal, there is vacuum level alignment at the nanowire and air interface. But, the band alignment and Fermi level pinning at the metal/nanowire interface is markedly different when the metal over-layer is present. In presence of metal over-layer, due to pinning, the significant value of $\Delta\Phi_B$ must be caused by some charge transfer. Bearing in mind the large charge transfer distance, the absolute magnitude of the transferred charge could be comparably small to yield the necessary shift of the levels. Thus, we propose that the interface states can be ionized by injected hot electrons which result in the emptying the interface. This ionization of interface states changes the Fermi level so that it effectively behaves like a small forward bias and hence the band bending as well as Schottky barrier height decreases. Fig. 8 shows the schematic band diagram of Au/ZnO nanowire Schottky diode under zero bias and a forward bias voltage. The experimental identification of tunneling, thermionic emission and other components for barrier height lowering predicts that the Fermi level deepening at Au-ZnO nanowire interface may originate from the ionization of interface states by injected hot electrons.

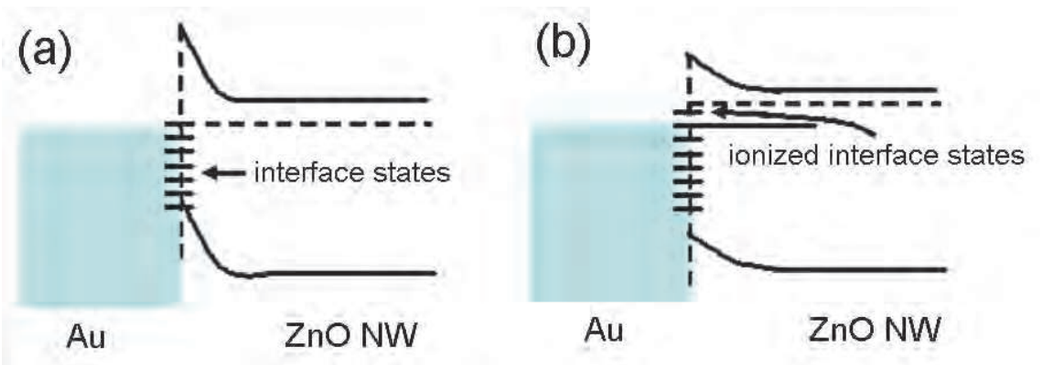

Fig. 8. Schematic band diagram of Au/ZnO NW Schottky diode (a) under zero bias and (b) with a forward bias.

4. Application

4.1 UV detector

A nanodevice unit made from single one-dimensional (1D) nanostructure, such as nanowire or nanobelt, attracts substantial research interests because it can provide a unique platform for fundamental investigations and also can serve as the building block for more

complicated device systems in nano- and microscale, for example, sensors, diodes and transistors (Lee et al., 2010; Zhou et al., 2008). Surface plays a crucial role to determine the electrical and optoelectronic properties of materials with a dimension of nanometer scale. There are several wide bandgap semiconducting materials for UV detection like GaN, ZnO, AlGaN (Munoz et al., 2001; Soci et al., 2007; Li et al., 2009). Because of their wide bandgap and high surface-to-volume ratio, nanoscale electronic devices have the potential to achieve high sensitivity and faster response for the UV detection. For a good UV detector, the growth of single crystalline ZnO nanowire is important. ZnO nanowires obtained from MOCVD technique shows a very good crystalline and optical property. As shown in Fig. (2), nanowires grown by MOCVD technique have two strong PL peaks at 382 and 388 nm, without any visible band emission. The sharp peaks presumably resulted from the excitons. Strong UV luminescence of free exciton recombination without any visible band emission is suitable for the UV laser device and visible blind UV detectors.

In past few years, enormous studies on UV detection have been conducted using ZnO nanowires, which were either fabricated with ohmic or Schottky contacts. However, most of these works are focused on the array of ZnO nanowires with few studies directed at the single nanowire (Li et al., 2009; Heo et al., 2004; Xu et al., 2006). In literature, it has been reported that single nanowires devices with both ohmic and Schottky contact have similar UV response characteristics even though the sensing mechanisms are different. The UV detection characteristics of Au/ZnO nanowire Schottky diode and the device with both side ohmic contacts were studied by measuring current-voltage (*I-V)* relationships with and without UV light (352 nm) (Fig. 9a). In the dark, *I-V* curve is asymmetric for the device with Schottly contact and linear for the device with both sides ohmic contact (inset). The nonlinearity of the *I-V* curve is caused by the Schottky barrier formed between the semiconductor and metal electrodes. For both devices, *I* increase with UV illumination.

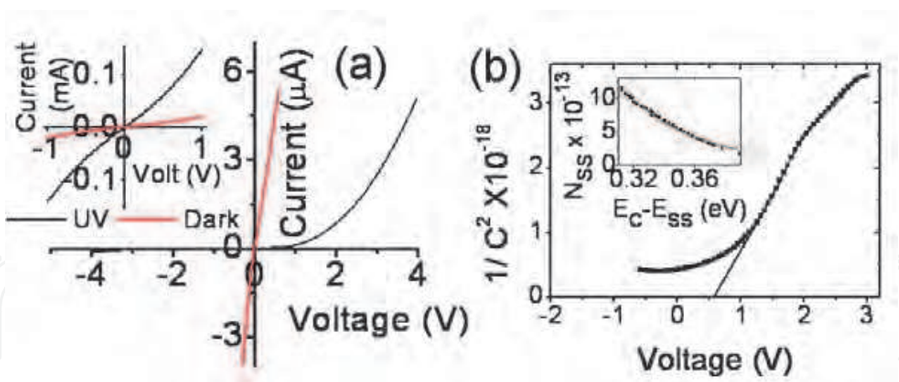

Fig. 9. (a) *I-V* characteristics for a representative Au/ZnO nanowire Schottky diode before and after UV illumination. The inset shows the *I-V* characteristics of a device with both side ohmic contacts. (b) Plot of ($1/C^2$) with *V* for Au/ZnO nanowires Schottky diode. The inset shows the density of interface states as a function of interface state energy ($E_C - E_{SS}$).

To test the reversibility of the sensor, the device was alternatively exposed to UV light and the corresponding current at a particular voltage (0.7 V and 0.3 V for the devices with both side ohmic contact and one side Schottky contact, respectively) was measured. For high-power UV illumination (25 mW/cm²), we have observed similar characteristics (sharp rise and sharp fall) for the devices with both sides ohmic and one side Schottky contact (not

shown here). But for low-power UV illumination (1.5 mW/cm^2), Figs. 10 (a) and (b) show the effect of NW surface and schottky barrier, respectively. Figure 10 (b) shows the photoresponse of the Schottky diode under the UV excitation at a forward bias of 0.3 V. The dark current was about 120 nA and the saturated photocurrent was about 9 μA under UV excitation. On the other hand, the NW device with both side ohmic contacts has the dark and the saturated photocurrent currents about 0.2 μA and 0.9 μA, respectively (Fig. 10 (a)). The photocurrent/dark current ratio is 75 for Schottky diode, which is superior to single NW UV detector (4.5) with both side ohmic contacts. Upon low-power UV excitation, the conductance of the Schottky diode was increased around two orders and to 80% of its saturation value within 1 s. When the UV light is turned off, the conductance was decreased to 85% of its saturation value within 1 s and recovered to its original dark level after 3 s. On the other hand, the device with both side ohmic contacts follows sharp but an exponential rise and exponential decay. It can be noticed that the current is reached almost the same value in each cycle and fully recovered for Schottky diode. But, both the dark and the saturated photo current level for the device with both side ohmic contacts increases with repeated exposure.

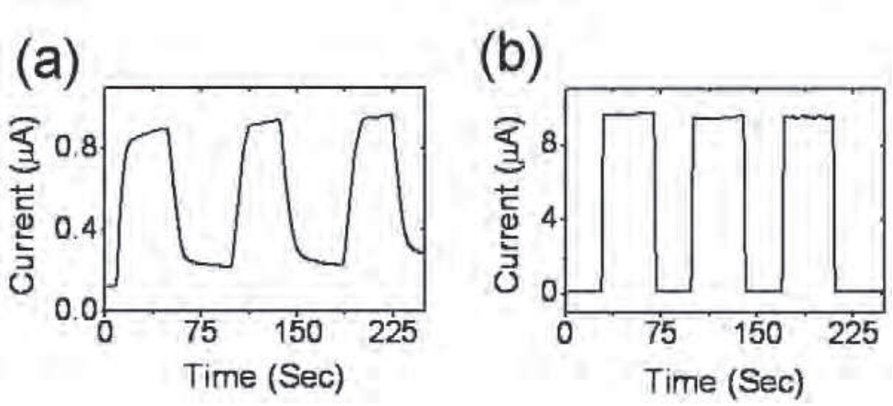

Fig. 10. UV response behaviors of the device with (a) both side ohmic contacts, (b) Schottky contact.

The interface density of states and surface states across the ZnO nanowire and Schottky contact may play a role in UV detection. To calculate the density of states at the interface of the Schottky diode, capacitance due to the depletion region was measured as a function of voltage and shown in Fig 9(b). The capacitance of a Schottky contact is related to the voltage by (Sze S. M., 1979)

$$C^{-2} = \frac{2\left[\Phi_{bi} - \left(E_C - E_F\right) - qV - kT\right]}{A^2 q \varepsilon_s N_d} \tag{6}$$

where Φ_{bi} is the barrier height, E_c is the conduction band edge, E_F is the Fermi level, ε_s is the permittivity of the semiconductor, A is area of contact and N_d is the carrier concentration. By plotting C^{-2} vs V and using eq (6), Φ_{bi} and N_d can be determined from the x-intercept and slope, respectively. The value of Φ_{bi} and N_d was 0.56 V and 2x10^{17}/cm^3, respectively. The barrier width (W) was obtained ~ 35 nm by using 2D Schottky barrier model (Sze S. M., 1979; Rhoderick, E. H., 1988)

$$W = \sqrt{\frac{2\varepsilon_s\left(\Phi_{bi} + V\right)}{qN_D}} \tag{7}$$

The Φ_{bi} (0.56 V) measured from *C*–*V* characteristics is higher than zero bias Φ_{bi} (0.4 V) obtained from temperature dependent *I*–*V* data by using generalized Norde method (Das et al., 2009). This offset is generally attributed to the image force lowering at the interface. Another possible cause to explain this discrepancy is the presence of an interfacial insulating layer. The value of ideality factor (*n*) was obtained 1.5 at 300 K. Generalized Norde's method has utilized the *I*–*V* characteristics in the low voltage region for the determination of the ideality factor and barrier height (Das et al., 2009). But in practice, the *n* values evaluated from the *I*–*V* characteristics in the forward bias region show voltage dependence. In such a case, the ideality factor *n(V)* is given by (Das et al., 2009)

$$n\left(V\right) = 1 + \frac{\delta}{\varepsilon_i}\left[\frac{\varepsilon_s}{W_D} + qN_{SS}\left(V\right)\right] \tag{8}$$

where, W_D is the space charge width, N_{SS} is density of states in equilibrium, δ is the thickness of the interfacial layer, ε_i is the permittivity of interfacial layer. The voltage-dependent ideality factors may be obtained from the slopes of *ln(I)* versus *V* plots in the forward bias region. The calculation of the density of surface states is complicated due to interfacial layer as neither ε_i nor δ is known. By considering δ = 0.5 nm and ε_i as that of free space, N_{SS} is calculated to be 6×10^{13} $cm^{-2}eV^{-1}$ at 0.3 V. The energy of the interface states with respect to the bottom of the conduction band at the surface of the semiconductor is given by (Das et al., 2009):

$$E_C - E_{SS} = q\left(\Phi_e - V\right) \tag{9}$$

with

$$\Phi_e = \Phi_b + \left(1 - \frac{1}{n\left(V\right)}\right)V \tag{10}$$

Density of interface states as a function of interface state energy ($E_C - E_{SS}$) for Au /ZnO NW Schottky diode is shown in the inset of Fig. 9(b). Exponential rise in the interface state density towards the bottom of the conduction band is very apparent. Low value of interface states signifies that the surface pinning of the Schottky barrier is low. Previously it has been shown that at equilibrium, the ionization of interface state by hot electron reduced the band bending as well as the Schottky barrier height. As the Schottky barrier height changes, a characteristic asymmetric conductance change is expected. Since, the density of surface state (6×10^{13} $cm^{-2}eV^{-1}$ at 0.3 V) is not very high and the change in current under the UV illumination is very high, visible light may not affect so much on the current.

The experimental observations on the two types of device structures are explicitly explained using schematics of the energy band diagrams of the nanowire surface and Schottky junction in the dark and under the UV illumination (Fig. 11). In ZnO, it is well known that in the dark oxygen molecules are adsorbed at the surface and capture free electrons and a low-

conductive depletion layer is formed near the surface (Soci et al., 2007). Upon UV illumination with photon energy larger than the semiconductor bandgap, electron-hole pairs are generated; holes migrate to the surface and discharge the negatively charged adsorbed oxygen ions and leaving behind unpaired electrons. Thus, band bending occurs and conductivity of the nanowire increases (Fig. 11 (a)). This hole-trapping mechanism through oxygen adsorption and desorption in ZnO nanowires augments the high density of trap states usually found in nanowires due to the dangling bonds at the surface and thus enhances the photoresponse. In case of single nanowire device, because of the higher exposed surface compared to array of nanowires, trapping at surface states drastically affects the transport and photoconduction property. Soci et al. reported that the oxygen adsorption and desorption at the nanowire surface occur in very short time (ns), suggesting that the desorbed oxygen molecules in air remain in close proximity to the surface and can be promptly re-adsorbed (Soci et al., 2007). This indicates that the oxygen re-adsorption to the surface and consequently the lowering of the photocurrent happen quickly after switching off the UV light; however, full recovery requires longer time, due to the time required for the diffusion of oxygen molecules.

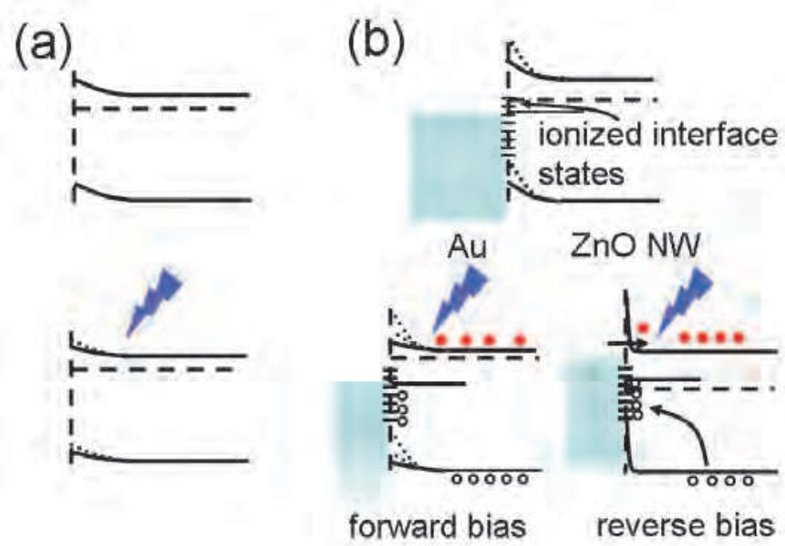

Fig. 11. Energy-level Diagram of (a) ZnO NW surface and (b) Au/ZnO NW interface.

Figure 11(b) shows the UV detection mechanism at the Schottky barrier. In Schottky device, both the forward and reverse current increase with UV exposure. It means that the photoexcited electron-hole pairs can greatly increase the concentration of majority carriers. We can therefore conclude that the barrier height is strongly modulated by the UV exposure. In forward bias, a large number of photogenerated electron-hole pair increases the majority carrier and ionizes the interface states. The ionization of interface states tends to increase the barrier height but, the large number of electron, generated due to the UV illumination, effectively reduces the barrier height under forward bias. As a result, band bending changes and current increases. Interface density of states play an important role in

reverse current. In reverse bias, holes are efficiently trapped by the interface states which shrink the depletion region and allow tunneling of electrons.

4.2 Hydrogen sensor

Hydrogen is a potential source of energy, which may replace the present fossil-based transportation fuels. It is also used as an important reagent in chemical industries. However, it is highly explosive above 4 vol % due to its low flash point (-253 °C) (Christofides et al., 1989). Accordingly, hydrogen leakage detection at early stage is not only necessary but also essential for safety. Solid-state hydrogen sensors based on pure Pt, Pd or Pd-containing alloys have been thoroughly explored as the interaction with hydrogen decreases the work function and increases resistance compared to pure material (Ibanez et al., 2006). Several other materials (SnO_2, InO_3, WO_3 and CNT) are currently being investigated for the active materials of sensors (Wang et al., 2006; Li et al., 2007). However, a high operation temperature is generally required for the better performance of the above mentioned sensors. Recently, there have been an increasing number of investigations on the exploration of selective materials to make the sensor more sensitive and reliable. In this concern, tremendous attentions have been focused on ZnO as a gas sensing material due to its high mobility of conduction electrons, good chemical and thermal stability under the operating conditions of sensors (Li et al., 2007; Wan et al., 2004). In addition, single crystalline nature, high mechanical strength, high temperature stability in oxygen ambient and ease of fabrication on several substrates by various techniques (Liao et al., 2008; Wan et al., 2004) are other advantage of ZnO nanostructures.

Single nanowire-based sensors are of particular interest as they can be fabricated by using conventional lithography technique. In addition to low cost and great miniaturization potential, the large surface to volume ratio and nanoscale dimension allow quick diffusion of gases into and from the nanostructure. Thus the rate of reaction increases, which leads to achieve higher sensitivity with faster response and recovery time. Nanoscale sensors also often provide a lower limit of detection due to a larger change in their electronic properties upon surface adsorption.

In case of ZnO nanostructure-based hydrogen sensor, the surface of the nanostructures plays a vital role. In that case, the contacts at the two ends are mostly chosen to be ohmic in order to enhance the change in conductance due to surface effect of the nanostructures. The surface-adsorbed gas molecules modify the electronic surface states and vary the electron concentration which is responsible for the change in conductivity of nanosensors (Liao et al., 2007). At room temperature, electrons released due to gas exposure are very less compared to the electron concentration in nanowire. Therefore, the relative change of conductance before and after gas exposure is small. Since the interaction energy of chemisorbed oxygen atom is large (1-10 eV), metal oxide gas sensors generally require high operating temperature (above 100 °C) to overcome the energy limits and achieve high sensitivity (Fan et al., 2009). However, the high operating temperature adversely affects sensor's reliability, durability and makes the sensors expensive with many complicated heating elements.

In order to improve the sensitivity at room temperature, we deliberately introduce a nonsymmetrical Schottky contact at one end of a ZnO single nanowire based nanodevice.

Here, the surface depletion layer controls the density and mobility of electrons in the nanowire, but the contact barrier controls the transport of electrons between the nanowire and electrode. As the width of the surface depletion is significantly smaller than the diameter of the nanowire, the surface depletion has little influence on the density and mobility of the electrons in the nanowire. However, the change in potential barrier at the Schottky contact greatly modifies the current conduction. The presence of impurities, inconsistencies and asymmetry in structure may alter the effective potential barrier and inhibit the flow of charge carriers, which may change the device characteristics. To solve this problem, defect free nanowires are required. In this communication, we have studied hydrogen-sensing properties of Pt/ZnO nanowire Schottky diodes by measuring current-voltage (*I-V)* relationships at different temperatures.

The sensitivity tests were carried out in a test chamber, where the change in current was measured at a fixed forward voltage (4 V) due to gas exposure. A known amount of highly purified hydrogen was injected from an ampoule along with argon gas acting as a diluting agent to get the required percentage (in ppm) of hydrogen in the measuring chamber. The sensing characteristics were then recorded at different temperatures with various hydrogen concentrations.

The sensitivity is defined as

$$S = \frac{I_G - I_{Ar}}{I_{Ar}} \tag{11}$$

where I_G and I_{Ar} are the currents in hydrogen and argon ambient, respectively. The above expression can be used for both the forward and reverse current modes at a fixed voltage. Fig. 12(*a*) shows the variation of sensitivity with hydrogen concentration at room temperature in the forward bias mode (4 V) for a representative device. One can observe that the sensitivity increases linearly with hydrogen concentration till 2000 ppm, beyond which it increases slowly and tends to saturate.

It seems that due to the increase in hydrogen concentration, more gas molecules are available to be in contact with the device. Thus, one would expect the response to increase up to a certain limit with increase in H_2 concentration as observed here. Afterwards, with the increase in concentration sensitivity tends to saturate. This may be due to a saturation of adsorption of hydrogen atoms at Pt/ZnO nanowire interface and lack of adsorbed oxygen ions at the nanowire surface to react with gas molecules. Consequently, time resolved sensitivity measurement has also been done. Fig. 12 (b) represents the variation of sensitivity with time, measured at room temperature (300 K), when the test gas (hydrogen at 2500 ppm) is introduced in the chamber. It is observed that the maximum sensitivity is obtained within 75 sec. After removal of the test gas, the sensor tends to come back to its initial state and this change is exponential. Sensitivity decreases fast for first 50 seconds and then slowly to its original state. Response time is defined as the time taken for the sensor to reach 90% of the saturation value after gas exposure. The above observation suggests that the response time in these devices is ~55 second. The response time for Pd/nano-GaN Schottky diode reported by Das *et al* (Das et al., 2007) was ~12 min. On the other hand, Rout *et al* [14] have observed a higher response time (~300 sec) by monitoring the change in conductivity due to hydrogen exposure. Thus, the response time of the single nanowire-based Schottky diode, studied here, is superior to those reported recently by other researchers (Das et al., 2007; Rout et al, 2007).

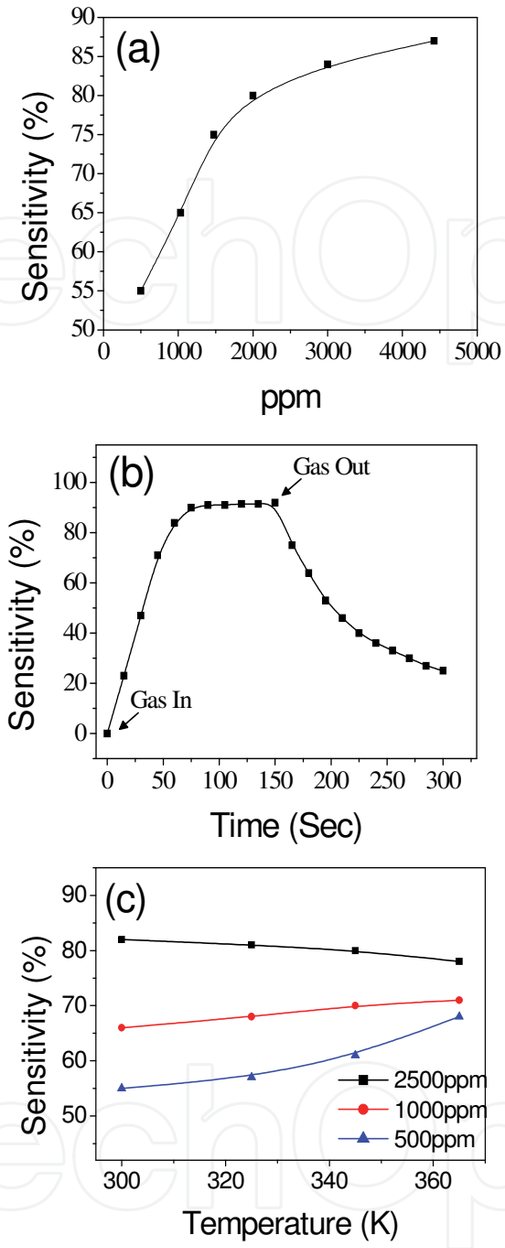

Fig. 12. (*a*) Variation of sensitivity with hydrogen concentration measured at room temperature in the forward current mode at 4 V. (*b*) Room temperature response behaviour for 2500 ppm of hydrogen. (c) Temperature dependent sensitivity for three representative hydrogen concentrations.

The contribution of ZnO nanowire surface and Pt/ZnO nanowire Schottky junction to the sensing mechanism was varied with gas concentration and temperature. In order to investigate the detail sensing mechanism, we have measured the sensitivity at different temperatures with different gas concentrations and plotted in Fig. 12(c). The measurements,

reported here, are taken at different temperatures after same interval (60 sec) of gas exposure after the equilibrium has been established. The sensitivity versus operating temperature curve shows a maximum at room temperature for 2500 ppm and decreases very slowly with increasing temperature, whereas it increases slowly but linearly with temperature for hydrogen concentration of 1000 ppm. On the other hand, for lower hydrogen concentration (500 ppm) sensitivity increases slowly up to 323 K. Beyond that appreciable change in sensitivity is observed. This can be explained by the temperature dependent adsorption and desorption process on both the nanowire surface and Schottky junction. Although individual contribution to the sensing mechanism is not distinguishable, but qualitatively one can explain the whole mechanism by considering change in band diagram in two different parts, namely ZnO nanowire surface and ZnO/Pt Schottky junction.

The hydrogen sensing mechanism, investigated in this study, is schematically shown in Fig. 13. Due to the geometry of the devices, the electric field near the junction between the ZnO nanowire and metal is much higher. As a result, the gases around the contact easily dissociate and ionized gases get adsorbed at ZnO/Pt Schottky junction even at room temperature. The change in Schottky barrier height is likely to be the most important for H_2 sensing but ZnO nanowire surface has also a contribution. However, this mechanism would be expected to exhibit a large dependence on the temperature and the concentration of gas around the devices. The sensing mechanism at nanowire surface can be explained in terms of the oxidizing/reducing gas effect. It is well known that the ZnO surface adsorbs oxygen species (O_2^-, O^{2-}, O^-) from air by trapping conductive electrons and makes the nanowire more resistive. Moreover, for a ZnO nanowire, high surface to volume ratio provides large number of surface atoms, which can lead to the insufficiency of surface atomic coordination and high surface energy (Liao et al., 2008). Therefore, the surface is highly active, which promotes further adsorption of oxygen from the atmosphere. On the other hand, when the nanowire is exposed to hydrogen environment, the reductive gas decreases the concentration of oxygen species on the nanowire surface, which in fact increases the electron concentration in the nanowire. It should be noted that the chemisorbed oxygen species depend strongly on temperature. Upon exposure to H_2, it is the chemisorbed surface oxygen ions that participate in the redox reaction preferably at higher temperature (Hudson J.B., 1998). The electrons, released from this process, are responsible for the change in electrical properties of ZnO nanowire through band bending. Thus, at higher temperatures, the nanowire surface will become more active for hydrogen sensing. On the other hand, the characteristic of the nanosensor is largely determined by the behavior at the Schottky junction. The electrical response comes from the variation of the Schottky barrier height and barrier width as a result of adsorption of gaseous species at the Schottky contact. The response due to adsorption can be explained from the band diagram at the metal/ nanowire contact. After the exposure to hydrogen, Pt adsorbs hydrogen by catalytic chemical adsorption. Some of the hydrogen atoms diffuse through the thin metal layer and form a dipole layer at the interface of metal-semiconductor contact, which reduces the Schottky barrier height (Schalwig et al., 2002). Although that may change the barrier width, it is the height of the barrier that matters significantly for charge transport at room temperature. As a result, both the forward and reverse current increases with the increase of the hydrogen concentration. However, the Pt surface gradually saturates with the increase in hydrogen concentration, so the rate of change of current decreases. When the gas ambient switched from hydrogen to air, the oxygen reacted with hydrogen and the resistance of the nanowires changed back to the original value. This is an attractive process for long term application of hydrogen sensor.

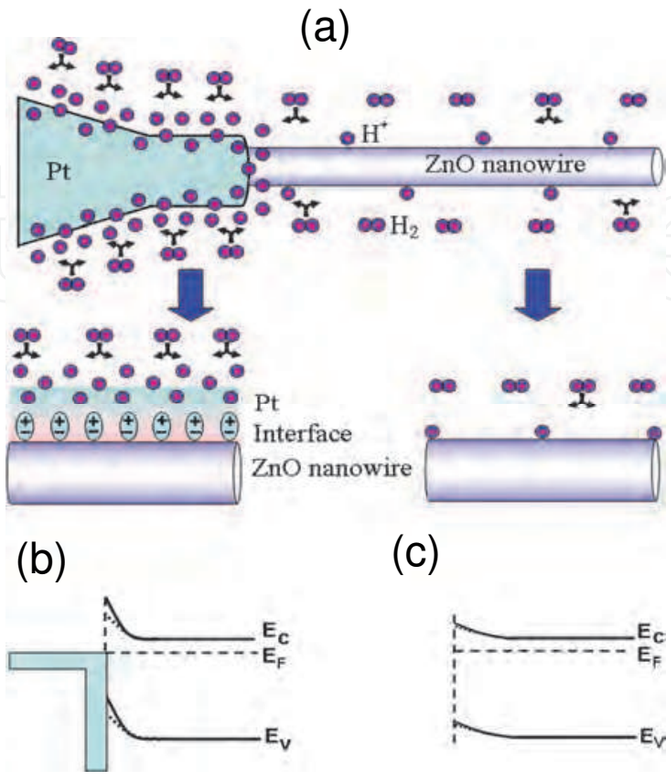

Fig. 13. (a) Schematic diagram of the Pt/ZnO single nanowire hydrogen sensing mechanism. Schematic energy level diagram of (b) Pt/ZnO nanowire interface and (c) ZnO nanowire surface.

The sensitivity depends on the combine effect of operating temperature and the hydrogen concentration. The Schottky barrier height increases with temperature, while it decreases with increase in hydrogen concentration. For higher hydrogen concentration (2500 ppm) the interface becomes saturated even at room temperature. This results a small change (decrease) in barrier height due to further adsorption of hydrogen atom with temperature, but the barrier height of the junction increases. As a result, the sensitivity decreases slowly with increase in temperature. But, for low hydrogen concentration (500 ppm), the interface does not saturate and more hydrogen can be adsorbed with increase in temperature. Thus, the sensitivity increases with increase in temperature for lower hydrogen concentration. Quick response and stability are also important characteristics of sensors. For quick response, the electron-exchange must take place rapidly so that equilibrium is established during measurement. As the Pt/nanowire interface is very small, a thin adsorbed hydrogen layer is formed quickly at the interface, which may block further electron exchange and thus equilibrium occurs. Hence, further increase in hydrogen concentration may eventually saturate the Pt/nanowire interface, which limits further electron-exchange. Thus, the interface of the Pt/ZnO nanowire Schottky device plays a significant role in quick response at room temperature hydrogen sensing.

5. Conclusion

In conclusion, Schottky dioded of single nanowire with different metal (Au, Ni and Pt) have been fabricated by e-beam lithography. Detailed I-V characteristics of the Schottky diodes have been investigated at different temperature. The barrier hight value and ideality factor at different temperature for different Schottky diodes were obtained from I-V measurements. The calculated barrier height value using generalized Norde method is in good agreement with the value obtained from XPS measurements. However, the calculated barrier height values are lower than theoretical value obtained from Schottky-Mott theory. The effect of tunneling, Fermi level pinning and image force lowering have contribution, but not enough to explain the barrier height lowering. The ionization of interface states by the injected hot electrons result in the emptying the interface states and consequent Fermi-level deepening at metal/semiconductor interface may be the possible reason for low barrier height. The single nanowire Schottky diodes were used for UV detector (Au/ZnO nanowire) and room temperature hydrogen sensor (Pt/ZnO nanowire). The schottky contact and ZnO surface yield unambiguous information on the UV detection mechanism, particularly in cases where the intensity of UV light is low. In case of Schottky diode, low power UV detection is significant. Hydrogen-sensing behavior of Pt/ZnO nanowire Schottky diode has suggested that it has good sensing characteristic ($S \approx 90\%$) at room temperature with a response time of ~55 s. The sensitivity shows a maximum at room temperature for H_2 concentration of 2500 ppm and decreases very slowly with an increase in temperature, whereas it increases slowly with temperature for H_2 concentration of 500 ppm.

6. References

Angadi, B., Park, H. C., Choi, H. W., Choi, J. W. & Choi, W. K. (2007). Oxygen plasma treated epitaxial ZnO thin films for Schottky ultraviolet detection. *J. Phys. D: Appl. Phys.*, Vol.40, pp. 1422.

Bengi, A., Altmdal, S., Ozcelik, S. & Mammadov, T.S. (2007). Gaussian distribution of inhomogeneous barrier height in $Al_{0.24}Ga_{0.76}As$/GaAs structures. *Physica B,* Vol. 396, pp. 22.

Chang, Y. C., Wu, H. W., Chen, H. L., Wang, W. Y. & Chen, L. J. (2009). Two-Dimensional Inverse Opal ZnO Nanorod Networks with Photonic Band Gap. *J. Phys. Chem. C*, Vol. 113, pp. 14778.

Christofides, C. & Mandelis, A. (1989), Operating characteristics and comparison of photopyroelectric and piezoelectric sensors for trace hydrogen gas detection. I. Development of a new photopyroelectric sensor. *J. Appl. Phys.*, Vol. *66*, pp. 3975

Coppa, B. J., Davis, R. F. & Nemanich, R. J. (2003). Gold Schottky contacts on oxygen plasma-treated, n-type ZnO(0001). *Appl. Phys. Lett.,* Vol. 82, pp. 400.

Das, S. N. & Pal, A. K. (2007), Hydrogen sensor based on thin film nanocrystalline n-GaN/Pd Schottky diode. *J. Phys. D: Appl. Phys.*, Vol. *40*, pp. 7291

Das, S. N., Sarangi, S. N, Sahu, S. N. & Pal, A. K. (2009), Metal Contacts in Nanocrystalline n-Type GaN: Schottky Diodes. *J. Nanosci. Nanotechno.* Vol. 9, pp. 2532

Das, S. N., Kar, J. P., Choi, J. H., Byeon, S., Jho, Y. D. & Myoung, J. M. (2009), Influence of surface morphology on the optical property of vertically aligned ZnO nanorods. *Appl. Phys. Lett.*, Vol. 95, pp. 111909.

Dhananjay, Nagaraju, J. & Krupanidhi, S. B. (2007), Investigations on magnetron sputtered ZnO thin films and Au/ZnO Schottky diodes. *Physica B*, Vol. 391, pp. 344.

Fan, S. W.; Srivastava, A. K. & Dravid, V. P. (2009) UV-activated room-temperature gas sensing mechanism of polycrystalline ZnO. *Appl. Phys. Lett.*, Vol. *95*, pp. 142106.

Fonoberov, V. A., Alim, K. A., Balandin, A. A., Xiu, F. & Liu, J. (2006). Photoluminescence investigation of the carrier recombination processes in ZnO quantum dots and nanocrystals. *Phys. Rev. B,* Vol.73, pp. 165317.

Hsu, H.C., Cheng, C.S., Chang, C.C., Yang, S., Chang, C.S. & Hsieh, W.F. (2005). Orientation enhanced growth and optical properties of ZnO nanowires grown on porous silicon substrates, *Nanotechnology*, Vol. 16, pp. 297.

Ievtushenko, A., Karpyna, V., Lashkarev, G., Lazorenko, V., Baturin, V., Karpenko, Lunika, A. M. & Danko, A. (2008). Multilayered ZnO films of improved quality deposited by magnetron sputtering, *Acta Phys. Pol. A*, Vol. 114, pp. 1131.

Heo, Y. W., Tien, L. C., Norton, D. P., Pearton, S. J., Kang, B. S., Ren, F. & LaRoche, J. R., (2004), Pt/ZnO nanowire Schottky diodes. *Appl. Phys. Lett.* Vol. 85, pp. 3107

Hudson, J. B. 1998 *Surface Science* (Wiley, New York).

Ibanez, F. J. & Zamborini, F. P. (2006) Ozone- and Thermally Activated Films of Palladium Monolayer-Protected Clusters for Chemiresistive Hydrogen Sensing. *Langmuir*, Vol. *22*, pp. 9789

Kar, J.P., Lee, S.W., Lee, W. & Myoung, J.M. (2008). Effect of sputtered films onmorphology of vertical aligned ZnO nanowires, *Appl. Surf. Sci.* Vol. 254, pp. 6677.

Kar, J.P., Ham, M.H., Lee, S.W. & Myoung, J.M. (2009). Fabrication of ZnO nanostructures of various dimensions using patterned substrates, *Appl. Surf. Sci.*, Vol. 255, pp. 4087.

Lee, T. I., Choi, W. J., Moon, K. J., Choi, J. H., Kar, J. P., Das, S. N., Kim, Y. S., Baik, H.K. & Myoung, J. M. (2010). Programmable Direct-Printing Nanowire Electronic Components. *Nano Lett.,* Vol. 10, pp. 1016.

Li, C. C.; Du, Z. F.; Li, L. M.; Yu, H. C.; Wan Q. & Wang, T. H. (2007), Surface-depletion controlled gas sensing of ZnO nanorods grown at room temperature. *Appl. Phys. Lett.*, Vol. *91*, pp. 032101.

Li, Y., Valle, F. D., Simonnet, M., Yamada, I. & Delaunay, J. J. (2009) High-performance UV detector made of ultra-long ZnO bridging nanowires. *Nanotechnology*, Vol. 20, pp. 045501

Liao, L.; Lu, H. B.; Li, J. C.; He, H.; Wang, D. F.; Fu, D. J.; Liu, C. & Zhang, W. F. (2007), Size Dependence of Gas Sensitivity of ZnO Nanorods *J. Phys. Chem. C*, Vol. *111*, pp. 1900.

Liao, L.; Lu, H. B.; Shuai, M.; Li, J. C.; Liu, Y. L.; Liu, C.; Shen, Z. X. & Yu, T. (2008), A novel gas sensor based on field ionization from ZnO nanowires: moderate working voltage and high stability. *Nanotechnology*, Vol. 19, pp. 175501.

Lin, Y. J. (2005). Application of the thermionic field emission model in the study of a Schottky barrier of Ni on p-GaN from current–voltage measurements. *Appl. Phys. Lett.,*Vol. 86, pp. 122109.

Liou, S.C., Hsiao, C.S. & Chen S.Y. (2005). Growth behavior and microstructure evolution of ZnO nanorods grown on Si in aqueous solution. *J. Cryst. Growth*, Vol. 274, pp. 438.

Munoz, E., Monroy, E., Pau, J. L., Calle, F., Omnes, F. & Gibart, P. (2001), III nitrides and UV detection. *J. Phys.: Condens. Matter,* Vol. 13, pp. 7115

Norton, D. P., Heo, Y. W., Ivill, M. P., Ip, K., Pearton, S. J., Chisholm, M. F. & Steiner, T. (2004). ZnO: growth, doping & processing. *Mater. Today,* Vol. 7, pp. 34, ISSN

Rout, C. S., Kulkarni, G. U., Rao, C. N. R. (2007), Room temperature hydrogen and hydrocarbon sensors based on single nanowires of metal oxides. *J. Phys. D: Appl. Phys.*, Vol. *40*, pp. 2777

Rhoderick, E. H. & Williams, R. H. (1988), *Metal-Semiconductor Contact* (Clarenoon, Oxford).

Schalwig, J.; Muller, G.; Karrer, U.; Eickhoff, M.; Ambacher, O.; Stutzmann, M.; Gorgens, L.& Dollinger, G. (2002), Hydrogen response mechanism of Pt–GaN Schottky diodes. *Appl. Phys. Lett.*, Vol. *80*, pp. 1222

Soci, C., Zhang, A., Xiang, B., Dayeh, S. A., Aplin, D. P. R., Park, J., Bao, X. Y., Lo, Y. H. & Wang, D. (2007), ZnO Nanowire UV Photodetectors with High Internal Gain. *Nano Lett.*, Vol. 7, pp. 1003

Sze, S. M. (1979). *Physics of Semiconductor Devices* (Wiley: New York).

Tsai,C. L., Lin, Y. J., Chin, Y. M., Liu, W. R., Hsieh, W. F., Hsu, C. H. & Chu, J. A. (2009). Low-resistance nonalloyed ohmic contacts on undoped ZnO films grown by pulsed-laser deposition. *J. Phys. D: Appl. Phys.* Vol. 42, pp. 095108

Wan, Q., Li, Q. H., Chen, Y. J., Wang, T. H., He, X. L., Gao, X. G. & Li, J. P. (2004), Positive temperature coefficient resistance and humidity sensing properties of Cd-doped ZnO nanowires. *Appl. Phys. Lett.* Vol. *84*, pp. 3085

Wan, Q., Li, Q. H., Chen, Y. J., Wang, T. H., He, X. L., Li, J. P. & Lin, C. L. (2004), Fabrication and ethanol sensing characteristics of ZnO nanowire gas sensors. *Appl. Phys. Lett.*, Vol. *84,* pp. 3654

Wang, C., Chu, X. & Wu, M. (2006), Detection of H_2S down to ppb levels at room temperature using sensors based on ZnO nanorods. *Sensors and Actuators B*, Vol. 113, pp. 320.

Werner, J.H. & Guttler, H.H. (1991). Barrier inhomogeneities at Schottky contacts. *J. Appl. Phys.*, Vol. 69, pp. 1522.

Xu, Q.A., Zhang, J.W., Ju, K.R., Yang, X.D. & Hou, X. (2006), ZnO thin film photoconductive ultraviolet detector with fast photoresponse. *Journal of Crystal Growth*, Vol. 289, pp. 44

Zhang, H. Z., Sun, X. C., Wang, R. M. & Yu, D. P. (2004). Growth and formation mechanism of *c*-oriented ZnO nanorod arrays deposited on glass. *J. Cryst. Growth*, Vol. 269, pp. 464.

Zhang, J., Zhang, L. D., Wang, X. F., Liang, C. H., Peng, X. S. & Wang, Y. W. (2001). Fabrication and photoluminescence of ordered GaN nanowire arrays. *J. Chem. Phys.*, Vol. 115, pp. 5714.

Zhou, J., Gu, Y., Fei, P., Mai, W., Gao, Y., Yang, Bao, R., G. & Wang, Z. L. (2008). Flexible Piezotronic Strain Sensor. *Nano Lett.* Vol. 8, pp. 3035.

Nanowires - Fundamental Research

Edited by Dr. Abbass Hashim

ISBN 978-953-307-327-9
Hard cover, 552 pages
Publisher InTech
Published online 19, July, 2011
Published in print edition July, 2011

Understanding and building up the foundation of nanowire concept is a high requirement and a bridge to new technologies. Any attempt in such direction is considered as one step forward in the challenge of advanced nanotechnology. In the last few years, InTech scientific publisher has been taking the initiative of helping worldwide scientists to share and improve the methods and the nanowire technology. This book is one of InTechâ€™s attempts to contribute to the promotion of this technology.

How to reference

In order to correctly reference this scholarly work, feel free to copy and paste the following:

Sachindra Nath Das, Jyoti Prakash Kar and Jae-Min Myoung (2011). Junction Properties and Applications of ZnO Single Nanowire Based Schottky Diode, Nanowires - Fundamental Research, Dr. Abbass Hashim (Ed.), ISBN: 978-953-307-327-9, InTech, Available from: http://www.intechopen.com/books/nanowires-fundamental-research/junction-properties-and-applications-of-zno-single-nanowire-based-schottky-diode

INTECH
open science | open minds

InTech Europe
University Campus STeP Ri
Slavka Krautzeka 83/A
51000 Rijeka, Croatia
Phone: +385 (51) 770 447
Fax: +385 (51) 686 166
www.intechopen.com

InTech China
Unit 405, Office Block, Hotel Equatorial Shanghai
No.65, Yan An Road (West), Shanghai, 200040, China
中国上海市延安西路65号上海国际贵都大饭店办公楼405单元
Phone: +86-21-62489820
Fax: +86-21-62489821

IntechOpen